Laser and Particle Beams (2005), *23*, 337–343. Printed in the USA.

DOI: 10.1017/S0263034605050482

Ion acceleration with ultrafast laser driven water droplets*

M. SCHNÜRER, S. TER-AVETISYAN, S. BUSCH, E. RISSE, M.P. KALACHNIKOV,
W. SANDNER, AND P.V. NICKLES
Max-Born-Institut, Berlin, Germany

(RECEIVED 14 October 2004; ACCEPTED 16 December 2004)

Abstract

Small water droplets (20 micron in diameter) have been exposed to intense ($\sim 10^{19}$ W/cm^2) laser pulses in order to study ultrashort ($\sim$ 35 fs) laser pulse driven ion acceleration. Ion emission spectra registered simultaneously in forward and backward direction in respect to the incident laser beam carry similar integral ion energy but show different ion cutoff energies. With simple model estimations on basis of the confined and spherical geometry of the droplet-target, we inferred acceleration field strengths of about (0.7–2) MV/μm. Up to 9% of the incident laser energy is converted to kinetic energy of ions, which have been accelerated to energies above 100 keV and up to 1.5 MeV. A laser pedestal at an intensity of about 10^{-7} of the peak intensity at 1–2 ns in front of the pulse peak still limits the achievable cutoff energies of emitted protons from the droplet. The observed increase of cutoff energies with an enhanced temporal contrast of the laser pulse is elucidated within a simple acceleration model.

Keywords: Ion acceleration; Laser plasma; Laser-plasma dynamics

1. INTRODUCTION

With the advent of the chirped pulse amplification (CPA) lasers (Strickland & Mourou, 1985) and its further development, new perspectives of efficient laser driven particle acceleration were opened (Bauer, 2003; Deutsch, 2003; Magunov *et al.*, 2003). In general, these processes relied on the fact that matter can be highly excited with intense light fields, using a moderate amount of energy within an ultrashort time interval. The laser pulse energy is efficiently transferred to hot electrons and a strong charge field is built up which in turn can accelerate ions to higher energies. The kinetic energy of these fast moving ions can approach several tens of MeV (Malka, 2002; Mourou *et al.*, 1998; Nakajima, 2000), which is a significant part of the incident laser energy. This striking feature has actuated already a broad variety of work concerning the study of underlying physical processes and possible application. Especially proton beams with particle energies of several MeV have a large potential for imaging of dense plasmas (Borghesi *et al.*, 2001, 2005). Further possible applications are techniques using nuclear activated samples (Santala *et al.*, 2001; Yamagiwa & Koga 1999) which rely on proton energy and average beam flux.

Huge electric fields produced by charge separation during relativistic laser matter interaction are discussed in this paper within the framework of different mechanisms, for instance, ponderomotive expulsion of electrons and the so-called "target normal sheath acceleration" (TNSA) (Hatchett *et al.*, 2000). At a typically produced field strength of 1 MV/μm (Hegelich *et al.*, 2002) a proton at rest needs about 470 fs to be accelerated to an energy level of 10 MeV. But the laser pulse does not need to be long because the lifetime of the acceleration field is determined by electron dynamics in the plasma, and can thus exceed the laser pulse duration. Recently, experiments (Mackinnon *et al.*, 2002) and simulations (Dong *et al.*, 2003) have shown the enormous potential of laser pulses with a high temporal contrast for laser driven ion acceleration. Several applications need a certain flux, which is connected with the pulse repetition rate and the target debris problem. Up to now, optimization of laser–target concepts in terms of laser energy consumption and temporal pulse parameters motivate further investigations.

In this paper, we will report on interaction studies focusing on proton and deuteron acceleration from isolated targets. Ultrashort intense laser pulses with duration shorter than the anticipated acceleration time for MeV-protons are exposed to single water droplets (Karsch *et al.*, 2003;

Address correspondence and reprint requests to: Dr. Ter-Avetisyan Sargis, Max-Born-Institut, Max-Born-Str. 2a, D12489 Berlin. E-mail: sargis@mbi-berlin.de
*This paper was presented at the 28th ECLIM conference in Rome, Italy.

Ter-Avetisyan *et al.*, 2004), and we put emphasis on the determination of specific parameters of the ion acceleration process.

2. EXPERIMENT

The experiments were carried out with 35 fs laser pulses at 810 nm center wavelength from the MBI-high-field-Ti:Sa-laser (Kalachnikov *et al.*, 2002). For the present experiments, up to 800 mJ pulses in a beam of 70 mm in diameter are focused with an f/2.5 off axis parabolic mirror. Interaction intensities of $\sim 10^{19}$ W/cm^2 were estimated from the energy content in a focal area with a diameter of ~ 6 μm. A commercially available capillary nozzle (Micro Jet Components, Sweden) is used as a target source. With the nozzle, liquid water or heavy water is injected into the vacuum chamber. The water jet decomposes after a few millimeter of propagation into a train of droplets which were well characterized (Düsterer, 2003; Hemberg *et al.*, 2000). The droplet diameter is about 20 μm. The laser is focused at about 10 mm below the jet nozzle outlet. For our studies, two identical Thomson parabola spectrometer registered the ion emission at observation angles of 0° (laser propagation direction), and 135°. The spectrometer entrance pinholes with a diameter of 200 μm are placed at a distance of 35 cm from the source. Microchannel-plates (MCP) were used for ion detection.

3. LASER ENERGY TO ION KINETIC ENERGY TRANSFORMATION

Figure 1 shows an example of a proton spectrum obtained from an irradiated droplet. Ion numbers were calculated with the single particle response factor of the MCP-CCD (charge-couple-device), detection assuming an isotropic ion emission from the droplet. This assumption is justified within a determined limit by previous experimental observations: Simultaneous registration of the ion emission with four Thomson spectrometers and covering an observation angle of 135 degree gave a signal variation within a factor of 2 to 3 (Busch *et al.*, 2003). Furthermore, the integral ion emissions were validated in experiments studying fusion generation in heavy water droplets (Schnürer *et al.*, 2004*a*). Averaging over several 10^4 shots, a conversion of about 2% of the incident laser energy on target into deuterons kinetic energy above 20 keV could be deduced from the determined ion emission.

An energy level of up to 9% was deduced from laser energy compared to proton kinetic energy within 120 keV and 1 MeV, and about 3% from laser energy to all oxygen ions with energies between 40 keV and 800 keV could be deduced. These values are above conversion ratios for MeV-ions at about 1%, which were obtained with an order of magnitude longer (several 100 fs up to 1 ps), and more energetic (10 J–50 J) laser pulses (e.g., Hegelich *et al.*, 2002). The comparison relates to an energy interval of the ions between the cutoff energy down to about 10% of the cutoff energy. Figure 1 shows the proton spectrum in a logarithmic; linear plot. Clearly two branches of the spectrum are visible which one can assign to proton-temperature parameters, 170 ± 20 keV and 630 ± 20 keV, respectively, if an exponential fit of each branch is done. A weighted average of the two branches of about 370 keV would follow.

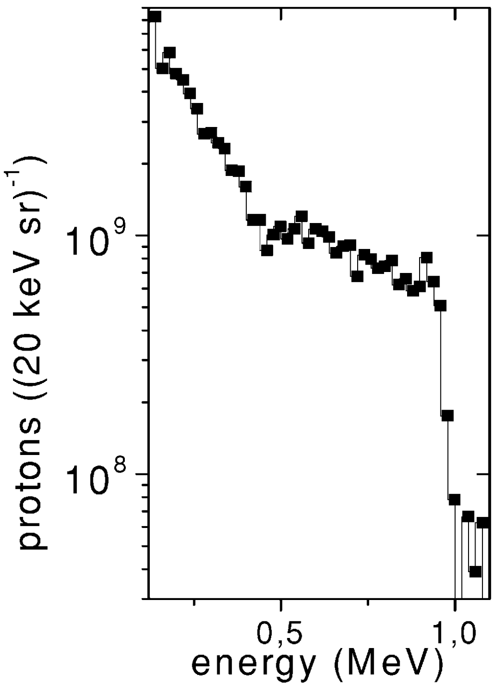

Fig. 1. Proton emission from a 20 micron H_2O-droplet exposed with a single laser pulse. Proton emission at 135° (cf. text).

Both populations are separated by a "dip" in the spectrum at about 450 keV. The occurrence of such dips is a relevant feature under our conditions, and is discussed on the basis of an expansion model (Wickens *et al.*, 1978), in more detail see Busch *et al.* (2004) and Ter-Avetisyan *et al.* (2004). In this model, briefly, the dip in the velocity distribution corresponds to an internal electrostatic sheath appearing due to hot- and cold-electron isothermal expansion, where ions are strongly accelerated in a small region. This dip develops in a region where the ions experience rapid acceleration due to an abrupt increase in the electric field. The dips in proton spectra emitted from water droplets vary in its position and its modulation depth, which we ascribe to small fluctuations in laser parameters as the beam is pointing on the droplet. We observed dips throughout the whole range of proton energies registered with our spectrometer. In recent theoretical studies, multispecies plasma effects and the influence of electron cooling are discussed (Bychenkov *et al.*, 2004).

Our result shows that laser pulses, which are shorter than the anticipated acceleration time of ions, can establish an efficient acceleration. The acceleration parameters for the present experimental conditions will be derived with a simple estimation.

4. CORRELATED ION EMISSION FROM A DROPLET

From the equations of motion it follows that an ion with mass m_{ion} and charge q can acquire a kinetic energy of $W_{kin} = q^2 E_{acc}^2 / (2\, m_{ion})\, t_{acc}^2$ in the E_{acc} electrostatic field during an acceleration time t_{acc}. From a symmetrical target like a sphere, which is uniformly excited, one would expect a perfect isotropic ion emission. Under our irradiation conditions, the target spheres are exposed by the laser from one side, which could initiate non-isotropic conditions. This has been looked at in more detail with two Thomson-MCP-spectrometers in order to register synchronously the single pulse ion emission in "forward"-direction (corresponds to the laser propagation direction) and "backward"-direction (corresponds to an angle of 135° to the laser propagation direction). Such a combination of two obtained spectra is shown in Figure 2.

Here we traced the emission of energetic deuterons from driven heavy water (D_2O) droplets. The high-energy cutoff value of the deuterons emitted to the backward direction is about twice as much as the value in forward direction. On the other hand, the deuteron numbers per energy bin are higher for the forward emission. It is worth noting that this dependency is a general characteristic for the ion emission of water and heavy water droplets under our conditions. On basis of estimations of the electron density in our confined droplet target (Busch *et al.*, 2003), and the laser energy conversion in hot electrons (Schnürer *et al.*, 2000*b*), we can derive acceleration field strength of 0.7 to 2 MV/μm (cf. Busch *et al.*, 2003).

Different ion energies can result from different acceleration field strengths and variations in the acceleration time. Because we focus the laser radiation on one side of the droplet (the front-side), one could easily assume that we can create due to the necessary propagation of the electrons, different hot electron populations in terms of energy, and

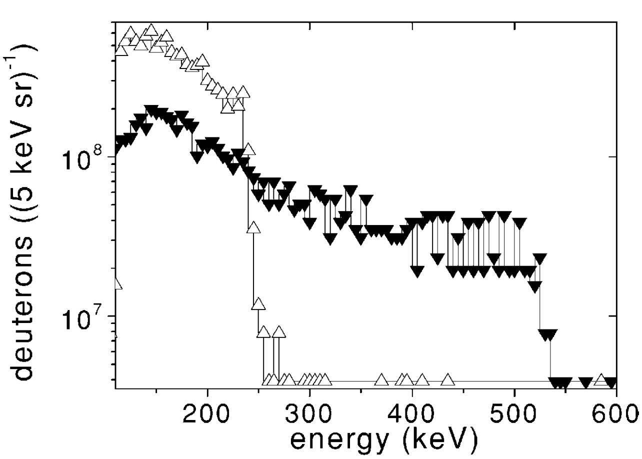

Fig. 2. Correlated deuteron emission from a 20 micron D_2O-droplet: Forward emission (in laser beam propagation direction)–empty triangles, backward emission (135° to laser beam propagation direction)–full triangles.

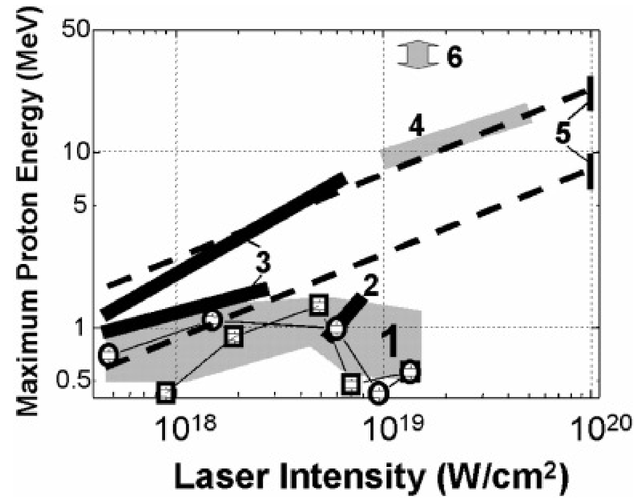

Fig. 3. Laser intensity dependence of cutoff-energies of laser-plasma accelerated protons: data points within area 1–this work, area 2–Spence *et al.* (2003), areas 3–Maksimchuk *et al.* (2000), Nemoto *et al.* (2001), area 4–Clark *et al.* (2000), Allen *et al.* (2003), areas 5–Mackinnon *et al.* (2002), theoretical prediction 6–Dong *et al.* (2003), *dashed* lines show a square-root scaling in respect to the laser intensity.

number density on the front- and back-side[1] of the target. On the other hand, as shown in Figure 2, the emitted number of deuterons per energy bin from the backside is higher. By integrating both spectra gives 0.26 mJ sr^{-1} and 0.27 mJ sr^{-1} for the backward- and forward-accelerated deuterons, respectively. These similar numbers show that the ion emission seems to be quite symmetrical concerning the term of energy transformation, and that the ion acceleration is driven by a hot electron population on both sides which is quite similar concerning its total energy.

The correlated ion-spectra will be an interesting benchmark for a complex computer modeling of small spherical targets in order to get a better insight into the acceleration scenario. A possible reason, propagation effects of the hot electrons in the target might become visible under our experimental conditions, caused by the ultrafast excitation of the hot electron population and its lifetime.

5. ION ACCELERATION IN DEPENDENCE ON LASER INTENSITY AND PULSE CONTRAST

The laser intensity was varied by changing both (1) the laser energy with an attenuator using the angular transmission dependence of polarizators in the system or (2) the laser pulse duration due to varying the grating separation in the pulse compressor. The observed cutoff dependence from laser intensity is shown in Figure 3. The shaded areas correspond to values measured from different experiments (see references in figure caption). The line guides the eye concerning a cut off energy scaling with the square root of the laser intensity.

[1]Backward accelerated ions originate from the front-side; forward acceleration refers to the backside (or rear-side).

https://doi.org/10.1017/S0263034605050482 Published online by Cambridge University Press

As visible, the maximum cutoff energies cannot be observed at the maximum incident laser intensity. At lower intensities, the cutoff energies scale approximately with the square root of the laser intensity, as it was observed in several other experiments which were additionally depicted in Figure 3, and which fit roughly to this intensity-scaling.

We assume that our observed brake-up of cutoff ion-energies at our highest intensities is connected with the temporal contrast of the laser pulse. Measurements with a third order correlator (Kalachnikov *et al.*, 2005) have quantified an ASE-pedestal of the pulse at a ~ ns time duration, with an intensity between 10^{-7} to 10^{-8} of the peak intensity (10^{18}–10^{19} W/cm^2), in dependence of pumping conditions of the laser amplifiers (Kalachnikov *et al.*, 2005). The resulting intensity of 10^{10}–10^{12} W/cm^2 is sufficient for producing different pre-plasma conditions on the vacuum-target interface, which influences the laser energy absorption, the resulting hot electron creation and the following ion acceleration. In the Appendix, we suggest a simple extension of Mora's ion-acceleration model (Mora, 2003), in order to infer a connection between the hot electron energy and the ion cutoff-energy. Thereby, ion-acceleration from an already heated surface provides lower energetic ions than from a cold one. This simple model shows how the ion energy is related to the ratio of the maximum electron energy (maximum Debye-length) and a start-energy of the electrons (start Debye-length). This start parameter is dependent on the pre-heating conditions. Different pre-heating of the target-surface can result from different laser pulse contrasts. Recently, ion acceleration from the rear-side of thin foils was investigated in dependence on foil thickness and laser pulse contrast (Kaluza *et al.*, 2004). Here we are looking to ions, which are accelerated from a laser-irradiated front-side of the target. Pre-heating provides a more extended pre-plasma with a reduced plasma density gradient. Such a situation was modeled with the one-dimensional LPIC++ (Lichters *et al.*, 1997) code. The calculated ion-spectrum becomes less energetic if due to a lower temporal laser pulse contrast, the high intensity peak of the pulse interacts with a more extended pre-plasma. This simple model can give some interpretation for our experimental findings concerning the ion spectra originating from the front-surface emitted in backward direction. In principle, a more complex scenario need to be modeled: In formed pre-plasma multi-dimensional effects as relativistic self focusing of the laser radiation can occur, which in turn increase the laser intensity and thus the hot electron energies. This can lead to an increase of the acceleration fields and corresponding ion energies at the rear-side of the target. Such effects are not covered by a one-dimensional modeling. But such effects, which have been seen with plane foil targets, have not been observed with the droplet target under our irradiation conditions.

In an additional experiment, we checked the dependence of the deuteron cutoff energy on the laser pulse contrast. We used the possibility that the ASE-level of the pumped Ti:Sa amplifier crystals can be modified by changing the temporal delay of the pump pulse. Doing so, a change of the ASE-pedestal level from 10^{-7} to (2–5) $\times$ 10^{-8} (intensity in relation to the pulse peak) was measured with a third order scanning autocorrelator (Kalachnikov *et al.*, 2005). This intensity ratio is an average value from several thousand of pulses while scanning the range between 300 ps to 10 ps in front of the pulse peak. With such a variation in the contrast ratio, we could observe a clear effect on the ion spectra. Two corresponding spectra recorded in backward emission direction are displayed in Figure 4.

It is clearly visible how the cutoff energy of the deuterons is shifted to higher energies if the temporal contrast ratio of the laser pulse is enhanced. Also the conversion of laser energy to ion kinetic energy is slightly enhanced if one compares the integrated spectra. In case of the laser shot with the higher contrast, the incident laser energy is reduced to about 70% (that is, ~ 500–600 mJ) because of the pump delay manipulation. Our experiments show how critical the temporal pulse contrast influences the ion spectra if ultrashort laser pulses are used. As an example, recent simulations with ultra-thin (40 nm) foils predict proton energies up to 40 MeV for a 50 fs laser pulse interaction at about 1.5×10^{19} W/cm^2 (Dong *et al.*, 2003). In order to exploit fully the capabilities of ultrashort laser pulses thin targets need to be used for increasing the energy density of the produced hot electrons and the related acceleration field strength. This behavior was experimentally demonstrated by Mackinnon *et al.* (2002) with sizing down the target thickness from several tens up to three microns. In order to pump targets having a ~ micron extension efficiently, a temporal contrast in the order of 10^{-10} must be envisioned, which keeps the target at a high density up to the interaction of the peak of the laser pulse.

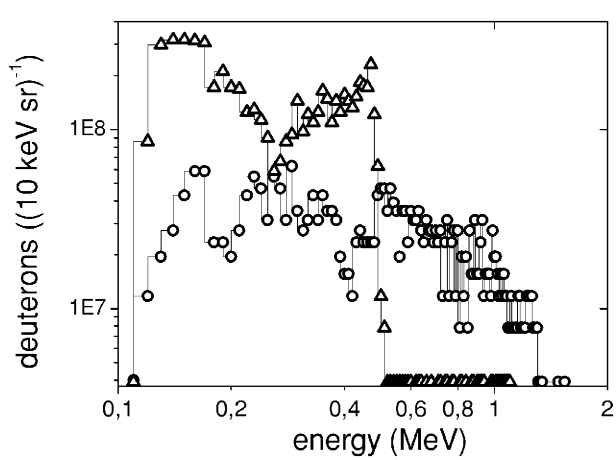

Fig. 4. Measured deuteron spectra from 20 micron D_2O-droplets in 135° backward emission in dependence of two different ASE-pedestal levels of the ultrashort pulse: triangles–contrast at maximum laser pulse energy, dots–reduced ASE-pedestal (values cf. text).

https://doi.org/10.1017/S0263034605050482 Published online by Cambridge University Press

6. SUMMARY

By exposing small water (H_2O or D_2O) droplets with ultrashort (~ 35 fs) and intense ($\sim 10^{19}$ W/cm^2) laser pulses, we could demonstrate a high conversion efficiency of several percent of the incident laser energy into kinetic energy of ions, which were accelerated to energies above 100 keV and up to 1.5 MeV. Taking advantage of the repetitive laser and the droplet target together with an online read-out of the signals from Thomson mass-spectrometers allowed us to study in detail the dependence of the ion acceleration on laser pulse energy, temporal pulse duration, and contrast. A temporal pulse contrast, of about 10^{-7} at 1 to 2 ns in front of the pulse peak, limits under our conditions the achievable cutoff energies of protons and deuterons. This is also visible in the brake-up of the cutoff energies if the full laser energy is supplied to the target. An increase of cutoff energies is observed with an enhanced temporal laser pulse contrast. A simple ion acceleration model for a pre-heated surface is suggested to account for this behavior, and also one-dimensional PIC-calculations show a cutoff lowering if an additional plasma ramp is introduced due to pre-heating. Correlated ion emission spectra in forward and backward direction in respect to the incident laser beam show different ion cutoff energies, but they carry similar integral ion energy. From simple model estimations, we inferred acceleration field strength of about 0.7–2 MV/μm. A further understanding of the experimental results needs more complex modeling as discussed here.

ACKNOWLEDGMENT

This work was partly supported by DFG-Project SFB-Transregio TR 18.

REFERENCES

Bauer, D. (2003). Plasma formation through field ionization in intense laser–matter interaction. *Laser Part. Beams* **21**, 489–495.

Borghesi, M., Audebert, P., Bulanov, S.V., Cowan, T., Fuchs, J., Gauthier, J.C., Mackinnon, A.J., Patel, P.K., Pretzler, G., Romagnani, L., Schiavi, A., Toncian, T. & Willi, O. (2005). High-intensity laser-plasma interaction studies employing laser-driven proton probes. *Laser Part. Beams* **23**, 291–295.

Borghesi, M., Bulanov, S., Campbell, D.H., Clarke, R.J., Esirkepov, T.Zh., Galimberti, M., Gizzi, L.A., MacKinnon, A.J., Naumova, N.M., Pegoraro, F., Ruhl, H., Schiavi, A. & Willi, O. (2001). Macroscopic evidence of soliton formation in multiterawatt laser-plasma interaction. *Phys. Rev. Lett.* **88**, 135002.

Busch, S., Schnürer, M., Kalashnikov, M., Schönnagel, H., Stiel, H., Nickles, P.V., Sandner, W., Ter-Avetisyan, S., Karpov, V. & Vogt, U. (2003). Ion acceleration with ultrafast lasers. *Appl. Phys. Lett.* **82**, 3354–3356.

Busch, S., Shiryaev, O., Ter-Avetisyan, S., Schnürer, M., Nickles, P.V. & Sandner, W. (2004). Shape of ion energy spectra in ultra-short and intense laser–matter interaction. *Appl. Phys. B* **78**, 911–914.

Bychenkov, V.Yu., Novikov, V.N., Batani, D., Tikhonchuk, V.T. & Bochkarev, S.G. (2004). Ion acceleration in expanding multispecies plasmas. *Phys. Plasmas* **11**, 3242–3250.

Clark, E.L., Krushelnick, K., Zepf, M., Beg, F.N., Tatarakis, M., Machacek, A., Santala, M.I.K., Watts, I., Norreys, P.A. & Dangor, A.E. (2000). Eergetic heavy-ion and proton generation from ultraintense laser-plasma interactions with solids. *Phys. Rev. Lett.* **85**, 1654–1657.

Deutsch, C. (2003). Transport of megaelectron volt protons for fast ignition. *Laser Part. Beams* **21**, 33–35.

Dong, Q.L., Sheng, Z.-M., Yu, M.Y. & Zhang, J. (2003). Optimization of ion acceleration in the interaction of intense femtosecond laser pulses with ultrathin foils. *Phys. Rev. E* **68**, 026408.

Düsterer, S. (2003). *Laser-Plasma Interaction in Droplet-Targets.* PhD Thesis. Jena: Friedrick-Schiller-University.

Hatchett, S.P., Brown, C.G., Cowan, T.E., Henry, E.A., Johnson, J.S., Key, M.H., Koch, J.A., Langdon, A.B., Lasinski, B.F., Lee, R.W., Mackinnon, A.J., Pennington, D.M., Perry, M.D., Phillips, T.W., Roth, M., Sangster, T.C., Singh, M.S., Snavely, R.A., Stoyer, M.A., Wilks, S.C. & Yasuike, K. (2000). Electron, photon, and ion beams from the relativistic interaction of petawatt laser pulses with solid targets. *Phys. Plasmas* **7**, 2076–2082.

Hegelich, M., Karsch, S., Pretzler, G., Habs, D., Witte, K., Guenther, W., Allen, M., Blazevic, A., Fuchs, J., Gauthier, J.C., Geissel, M., Audebert, P., Cowan, T. & Roth, M. (2002). MeV ion jets from short-pulse-laser interaction with thin foils. *Phys. Rev. Lett.* **89**, 085002.

Hemberg, O., Hansson, B.A.M., Berglund, M. & Hertz, H.M. (2000). Stability of droplet-target laser-plasma soft X-ray sources. *J. Appl. Phys.* **88**, 5421–5425.

Kalachnikov, M.P., Karpov, V., Schonnagel, H. & Sandner, W. (2002). 100-Terawatt titanium-sapphire laser system. *Laser Phys.* **12**, 368.

Kalachnikov, M.P., Risse, E., Schönnagel, H. & Sandner, W. (2005). Double chirped-pulse-amplification laser: A way to clean pulses temporally. *Optics Lett.* **30**, 923.

Kaluza, M., Schreiber, J., Santala, M.I.K., Tsakiris, G.D., Eidmann, K., Meyer-ter-Vehn, J. & Witte, K. (2004). Influence of the laser prepulse on proton acceleration in thin-foil experiments. *Phys. Rev. Lett.* **93**, 045003.

Karsch, S., Düsterer, S., Schwoerer, H., Ewald, F., Habs, D., Hegelich, M., Pretzler, G., Pukhov, A., Witte, K. & Sauerbrey, R. (2003). High-intensity laser induced ion acceleration from heavy-water droplets. *Phys. Rev. Lett.* **91**, 015001.

Lichters, R., Pfund, R.E.W. & Meyer-ter-Vehn, J. (1997). A parallel one-dimensional relativistic electromagnetic particle-in-cell code for simulating laser-plasma-interaction. Report MPQ 255. Berlin: Max-Planck-Institut für Quantenoptik, Garching.

Mackinnon, A.J., Sentoku, Y., Patel, P.K., Price, D.W., Hatchett, S., Key, M.H., Andersen, C., Snavely, R. & Freeman, R.R. (2002). Enhancement of proton acceleration by hot-electron recirculation in thin foils irradiated by ultraintense laser pulses. *Phys. Rev. Lett.* **88**, 215006.

Magunov, I., Faenov, A.Ya., Skobelev, I.Yu., Pikuz, T.A., Dobosz, S., Schmidt, M., Perdrix, M., Meynadier, P., Gobert, O., Normand, D., Stenz, C., Bagnoud, V., Blasco, F., Roche, J.R., Salin, F. & Sharkov, B.Yu. (2003). X-ray spectra of fast ions generated from clusters by ultrashort laser pulses. *Laser Part. Beams* **21**, 73–79.

Maksimchuk, A., Gu, S., Flippo, K., Umstadter, D. & Bychenkov, V.Yu. (2000). Forward ion acceleration in thin films driven by a high-intensity laser. *Phys. Rev. Lett.* **84**, 4108–4111.

Malka, V. (2002). Charged particle source produced by laser–plasma interaction in the relativistic regime. *Laser Part. Beams* **20**, 217–221.

Mora, P. (2003). Plasma expansion into a vacuum. *Phys. Rev. Lett.* **90**, 185002.

Mourou, G.A., Barty, C.P.J. & Perry, M.D. (1998). Ultrahigh-intensity lasers: Physics of the extreme on a tabletop. *Phys. Today* **51**, 22–28.

Nakajima, K. (2000). Particle acceleration by ultraintense laser interactions with beams and plasmas. *Laser Part. Beams* **18**, 519–528.

Nemoto, K., Maksimchuk, A., Banerjee, S., Flippo, K., Mourou, G., Umstadter, D. & Bychenkov, V.Yu. (2001). Laser-triggered ion acceleration and table top isotope production. *Appl. Phys. Lett.* **78**, 595–597.

Santala, M.I.K., Zepf, M., Beg, F.N., Clark, E.L., Dangor, A.E., Krushelnick, K., Tatarakis, M., Watts, I., Ledingham, K.W.D., McCanny, T., Spencer, I., Machacek, A.C., Allott, R., Clarke, R.J. & Norreys, P.A. (2001). Production of radioactive nuclides by energetic protons generated from intense laser-plasma interactions. *Appl. Phys. Lett.* **78**, 19–21.

Schnürer, M., Hilscher, D., Jahnke, U., Ter-Avetisyan, S., Busch, S., Kalachnikov, M., Stiel, H., Nickles, P.V. & Sandner, W. (2004*a*). Explosion characteristics of intense femtosecond-laser-driven water droplets. *Phys. Rev. E* **70**, 056401.

Schnürer, M., Nolte, R., Rousse, A., Grillon, G., Cheriaux, G., Kalachnikov, M.P., Nickles, P.V. & Sandner, W. (2000*b*). Dosimetric measurements of electron and photon yields from solid targets irradiated with 30 fs pulses from a 14 TW laser. *Phys. Rev. E* **61**, 4394–4401.

Spence, I., Ledingham, K.W.D., McKenna, P., McCanny, T., Singhal, R.P., Foster, P.S., Neely, D., Langley, A.J., Divall, E.J., Hooker, C.J., Clarke, R.J., Norreys, P.A., Clark, E.L., Krushelnick, K. & Davies, J.R. (2003). Experimental study of proton emission from 60-fs, 200-mJ high-repetition-rate tabletop-laser pulses interacting with solid targets. *Phys. Rev. E* **67**, 046402.

Strickland, D. & Mourou, G. (1985). Compression of amplified chirped optical pulses. *Opt. Commun.* **56**, 219–221.

Ter-Avetisyan, S., Schnürer, M., Busch, S., Risse, E., Nickles, P.V. & Sandner, W. (2004). Spectral dips in ion emission emerging from ultrashort laser-driven plasmas. *Phys. Rev. Lett.* **93**, 155006.

Wilks, S.C., Langdon, A B., Cowan, T.E., Roth, M., Singh, M., Hatchett, S., Key, M.H., Pennington, D., MacKinnon, A. & Snavely, R.A. (2001). Energetic proton generation in ultra-intense laser-sold interactions. *Phys. Plasmas* **8**, 542–549.

Wickens, L.M., Allen, J.E. & Rumsby, P.T. (1978). Ion emission from laser-produced plasmas with two electron temperatures. *Phys. Rev. Lett.* **41**, 243–246.

Yamagiwa, M. & Koga, J. (1999). MeV ion generation by an ultra-intense short-pulse laser: application to positron emitting radionuclide production. *J. Phys. D: Appl. Phys.* **32**, 2526–2528.

APPENDIX

In order to calculate the energy, an ion with charge Ze_0 and a mass m_i can acquire in a temporal varying electric field $E(t)$ we solve the equation of non-relativistic motion:

$$\frac{dv}{dt} = \frac{Ze_0 E(t)}{m_i}, \tag{1}$$

by integrating

$$v = \frac{Ze_0}{m_i}\int_{t_0}^{t} E(t)\,dt, \tag{2}$$

and $v - v_0 \equiv v$—velocity, t_0—start time.

Using Mora's (Mora, 2003) approach of a self similar electric field $E_{ss}(t) = kT_e/(e_0 c_s t)$ (kT_e–laser intensity dependent electron energy–hot electrons, $c_s = (ZkT_e/m_i)^{1/2}$–ion sound speed) which was created due to the intense laser driven charge displacement we have:

$$E(t) = \frac{(kT_e m_i)^{1/2}}{Z^{1/2} e_0 t}. \tag{3}$$

With (2) and (3) follows

$$v = \left(\frac{ZkT_e}{m_i}\right)^{1/2} \ln\left(\frac{t}{t_0}\right), \tag{4}$$

and for the ion-kinetic energy $E_{kin} = (m_i/2)v^2$ we obtain

$$E_{kin} = \frac{Z}{2} kT_e \ln^2\left(\frac{t}{t_0}\right). \tag{5}$$

The maximum possible time for gaining energy we identify with the flight time of the ion through the zone of the build-up electric field $E(t)$ which has the characteristic extension of the Debye–length

$$\lambda_D = \left(\frac{\varepsilon_0 kT_e}{e_0^2 n_e}\right)^{1/2}, \tag{6}$$

(ε_0–absolute permeability, n_e–electron density).

Because (5) becomes singular for $t_0 \to 0$ we set the start point t_0 at a low electron temperature $kT_{e\ cold}$ with a small $\lambda_{D\ cold}$ when the high intensity interaction begins. For an accelerated motion one has $t/t_0 = (s/s_0)^{1/2}$. So, finally using for the path length $s \equiv \lambda_D$ and (6) we arrive to

$$E_{kin} = \frac{Z}{2} kT_e \ln^2\left(\frac{kT_e}{kT_{ecold}}\right)^{1/4}. \tag{7}$$

The start parameter $kT_{e\ cold}$ can be interpreted as a measure of the pulse contrast. Low contrast yields higher $kT_{e\ cold}$ and less kinetic ion energy. As examples we would have from (7) with $Z = 1$,

https://doi.org/10.1017/S0263034605050482 Published online by Cambridge University Press

$kT_e = 600$ keV and $kT_{e\ cold} = 100$ eV: $E_{kin} \approx 2.4 \times kT_e = 1.4$ MeV for a 100 eV pre-plasma (low laser pulse contrast) and for $kT_{e\ cold} =$ 1 eV : $E_{kin} \approx 5.5 \times kT_e = 3.3$ MeV for a 1 eV pre-plasma (high laser pulse contrast). The possible parameter variation one can put in (7) covers a factor α, which is depending on different model approaches between 2 and 12 if $E_{kin} = E_{ion} = \alpha T_{hot} = \alpha kT_e$ is written in a simple scaling form (Wilks *et al.*, 2001). Here we suggest a simple modification how α could be influenced using a cold electron temperature-parameter of the surface from which the ions are accelerated.